

PARTICLE EMISSIVITY IN CIRCUMSTELLAR DISKS

STEVEN V. W. BECKWITH

Department of Astronomy, Space Sciences Building, Cornell University, Ithaca, NY 14853-6801

AND

ANNEILA I. SARGENT

Division of Physics, Mathematics, and Astronomy, California Institute of Technology, Pasadena, CA 91125

Received 1990 December 20; accepted 1991 May 6

ABSTRACT

Submillimeter continuum observations of 29 pre-main-sequence objects in Taurus and Orion are used to study the wavelength dependence of particle emission. These objects are mostly T Tauri stars whose long-wavelength emission is thought to originate in circumstellar disks. The flux densities imply power-law frequency distributions with spectral indices between 2 and 3 in almost all cases. If the emission is optically thin, the particle emissivities have power-law indices between -1 and 1 ; otherwise, these values are lower limits. We argue that in most cases the emission is optically thin at wavelengths near 1 mm, so the measured indices should be close to the true values. The indices derived for the circumstellar particles are substantially smaller than those thought to obtain in the diffuse interstellar medium and dense molecular clouds; they imply that the millimeter-wave opacities are *larger* near these stars than in the interstellar medium. Particle shape changes, possibly a result of particle growth, and composition changes, especially enhancements of iron-bearing compounds, can produce the observed behavior. The effect is to *decrease* the required amount of disk material needed to produce the observed millimeter-wave continuum emission.

Subject headings: stars: circumstellar shells — stars: mass loss — stars: pre-main-sequence

1. INTRODUCTION

Almost 50% of the nearby T Tauri stars are thought to have circumstellar disks similar in most respects to the primitive solar nebula (Beckwith et al. 1990, hereafter Paper I). At present, these are the only candidates for regions of ongoing planet-formation, and, as such, they provide a unique opportunity to gain an accurate picture of our own origins.

Precise knowledge of the total amount and distribution of matter is essential to assess the planet-forming properties of these young objects. The thermal radiation from solid particles detected at infrared and millimeter wavelengths provides the bulk of our information about their salient physical properties, the temperature distribution and total mass. A major uncertainty is introduced by the ill-defined mass opacity coefficient, κ_v , and its frequency dependence, usually assumed to follow a power law, $\kappa_v \propto \nu^\beta$. The values of κ_v and β bear strongly not only on the determination of disk masses, but also on the nature of the particles giving rise to the thermal emission; from studies of the opacity, it may even be possible to identify changes in particle properties commensurate with the onset of planetary birth.

A wide range of values for κ_v are to be found in the literature (see Paper I), and it is not at all obvious which is most appropriate for the warm, dense conditions in circumstellar disks. Current evidence suggests κ_v is different for the circumstellar particles than is conventionally assumed for dust in the interstellar medium (Beckwith et al. 1986; Sargent & Beckwith 1987; Adams, Emerson, & Fuller 1990; Weintraub, Sandell, & Duncan 1989; Paper I). The observed frequency dependence of particle emission at millimeter wavelengths is flatter than expected for typical interstellar particles in optically thin disks; the values for the emissivity index, β , are generally 1 or less. Such a change in κ_v might come about for several reasons, the most interesting of which would be particle growth in the

dense gas, eventually leading to the formation of very large particles or planets. This was presumably the way in which the solar system came to be.

The motivation for the present paper was to establish the frequency dependence of κ_v at millimeter wavelengths in the material surrounding young stars and thereby refine estimates of its absolute value. Millimeter-wave observations were made for 29 visible sources in the Taurus dark cloud. The long wavelengths are necessary to ensure that the emission is in the Rayleigh-Jeans limit with low optical depth. Our sample contains stars believed to have circumstellar disks similar to the primitive solar nebula based on the criteria described in Paper I: high far-infrared optical depths around *visible* stars, shallow spectral energy densities longward of $5 \mu\text{m}$, and large millimeter-wave flux densities indicative of $\geq 0.01 M_\odot$ of H_2 . Evidence for changes in particle composition, size, or shape, reflected in the emissivity index, could therefore be relevant to theories of cosmogony.

2. OBSERVATIONS

The observations were carried out at the Caltech Submillimeter Observatory (CSO) in Hawaii during 1989 November through December 4, and 1990 December 4 through 9. The detector was a silicon composite bolometer fed by a Winston cone and cooled to a few tenths of a degree with a ^3He refrigerator. The filtering employed standard techniques: a scattering filter of black polyethylene fused to fluorogold at 77 K blocked wavelengths in the far-infrared; a crystal quartz filter coated with black polyethylene at 4 K eliminated all near-infrared radiation; and bandpass filters, made of metal mesh on nylon or polyethylene, defined the actual wavebands (e.g., Whitcomb & Keene 1980; Cunningham 1982). Different Winston cones were used with each filter to match the diffraction limit of the 10 m telescope, giving different beam sizes on the sky.

TABLE 1
FILTER PARAMETERS

λ_0 (mm)	α	λ_{eff} (mm)	$\Delta\lambda$ (mm)	FWHM
1.1.....	-1	1.235	0.76	22"
	0	1.172	0.60	
	1	1.128	0.47	
	2	1.087	0.27	
	3	1.056	0.25	
0.8.....	-1	0.798	0.16	17
	0	0.792	0.17	
	1	0.783	0.16	
	2	0.777	0.19	
	3	0.769	0.19	
0.6.....	-1	0.630	0.062	13
	0	0.628	0.062	
	1	0.626	0.068	
	2	0.625	0.068	
	3	0.624	0.067	

Table 1 lists the filter parameters. Because the bandwidths of the filters are large and the telluric opacity quite variable over the passband, the effective wavelength of each filter depends on the spectral index, α , of the source. The effective wavelengths were derived by convolving power law spectra with the measured filter transmission characteristics (kindly provided to us by J. Keene) and known telluric absorption; they appear in the third column.

A pupil plane chopper provided for sky subtraction. Since almost all the continuum emission from these objects is unresolved in the CSO beam (Sargent & Beckwith 1987, 1989; Paper I), the chopper spacing was set to twice the beam diameter (FWHM) at each wavelength to minimize detection of more extended flux from the dark cloud. A lock-in amplifier demodulated the bolometer output, while a small computer recorded the demodulated signal.

The computer recorded data every 10 ms. Since the post-detection time constant was 125 ms, the output stream was heavily over sampled. Statistics of each 100 samples (1 s of data) gave a real-time measure of the noise, allowing automatic detection (and rejection) of spikes from the bolometer. Power spectra of the output stream from the preamplifier of the dewar also allowed us to monitor the relatively large microphonic interference and to set the chopper frequency to minimize this interference.

The objects Mars, W3(OH), CRL618, IRC + 10216, 3C 273, and 3C 84 provided standards to calibrate the flux density scale; the latter two sources are known to be variable, but observations of these objects with the Owens Valley interferometer within a few days of the 1989 CSO run (Scoville 1988, personal communication) established accurate flux densities at 2.7 mm. Mars and Uranus were below the horizon at the time of the 1989 observations. Table 2 lists the flux densities assumed for each of the standard calibrators at the effective wavelengths of observation. The object IRC + 10216 is known to be extended at these wavelengths, and we estimated flux densities appropriate to the beam sizes used at the CSO. The flux for Mars was calculated using the JCMT program kindly provided by C. J. Chandler.

The star HL Tauri was an excellent secondary standard. This object has been well measured at several submillimeter and millimeter wavelengths (e.g., Adams et al. 1990) and is close in the sky to most of our sample. Every third observation was of HL Tau. The repeated observations made it possible to

TABLE 2
ASSUMED FLUX DENSITIES

Calibrator	α	λ_{eff} (mm)	F_ν (Jy)
W3(OH)	3.0	1.056	13
CRL 618	1.6	0.780	3.1
		0.626	4.4
IRC + 10216	2.7	0.790	5.9
3C 273	-0.4	0.795	9
3C 84	-0.4	0.795	7
HL Tau	3.0	1.056	1.1
		0.770	3.2
		0.624	5.5

derive accurate air mass corrections for all the stars and monitor the opacity of the sky. A tipping radiometer also provided continuous measures of the zenith opacity at 1.3 mm throughout the run. In general, there was a good correlation between the opacity derived from the HL Tau measurements and the opacities indicated by the tipping radiometer. We attribute the remaining dispersion in the various observations of both the calibrator stars and HL Tau mainly to changing telluric opacity, especially at the short wavelengths.

Owing to the lack of strong, unresolved sources in the night sky at the time of the observations, it was difficult to calibrate the low level side lobes of the beams at each wavelength. Observations of HL Tau were used to normalize each night based on assumed flux densities derived from the observations of the standards; its derived flux density at each wavelength appears in Table 2. These correspond reasonably well to the values found by Adams et al. (1990). Our derived flux densities are somewhat low compared to theirs but by similar factors at each wavelength; therefore, the derived spectral indices should be similar to theirs.

Figure 1 shows the apparent flux of HL Tau at three different wavelengths as a function of air mass for three of the nights in 1989. These were typical of the entire run. On 1989 November 29, strong variations at the beginning of the night clearly indicated opacity changes in the atmosphere, and these data

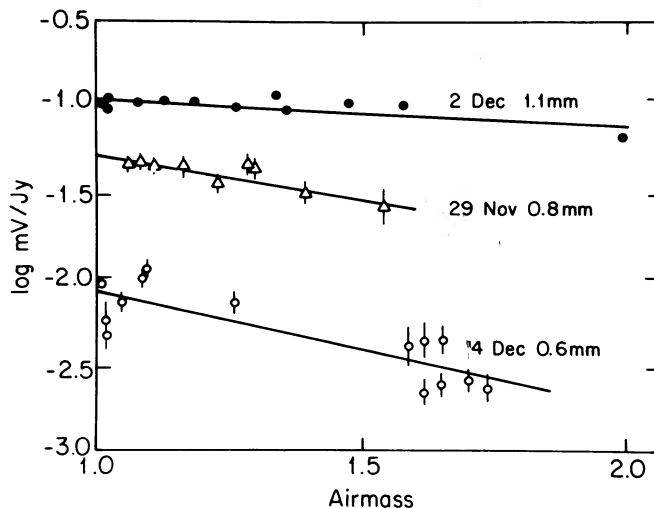


FIG. 1.—Apparent sensitivity of the bolometer as a function of air mass for the three wavelengths on different nights. Only statistical uncertainties are shown on each point. The straight lines are fits to the data assuming flux decreases exponentially with air mass.

TABLE 3

DERIVED AIR MASS CORRECTIONS AND CALIBRATION FACTORS

Date	λ (mm)	dex/AM	Jy mV ⁻¹	Transmission
1989 Nov 29.....	0.8	-0.451	26.5	35%
1989 Nov 30.....	0.8	-0.576	33.5	27%
1989 Dec 01.....	0.8	-1.210	29.6	6%
1989 Dec 02.....	1.1	-0.029	9.6	94%
1989 Dec 03.....	0.8	-0.547	26.9	28%
1989 Dec 04.....	0.6	-0.690	115	20%
1990 Dec 07.....	0.6	-0.384	62.3	41%
	0.8	-0.115	21.7	77%
	1.1	-0.078	33.3	84%
1990 Dec 08.....	0.6	-0.918	88.5	12%
	0.8	-0.450	24.5	35%
1990 Dec 09.....	0.6	-0.731	58.3	19%
	0.8	-0.387	19.7	41%
	1.1	-0.048	35.4	90%

were rejected. There were occasional pointing uncertainties as the result of winds. For this reason, we have assigned the data of 1989 December 3 much lower weight in the final results. The derived air mass corrections and calibration factors are given in Table 3.

3. RESULTS

Table 4 lists the observed flux densities of the sample stars. In general, there is excellent agreement between the CSO measurements at 1.1 mm and the 1.3 mm observations in Paper I, allowing for the wavelength dependence of the flux density. Our results for the sources in common with Adams et al. (1990) and Weintraub et al. (1989) are very similar to theirs. Although the air mass curve from HL Tau was smooth and linear, the 0.6 mm flux densities should be regarded with caution, since telluric fluctuations and systematic calibration uncertainties will be severe. On the other hand, the 1.1 and 0.8 mm observations should be reliable; repeated measurements of the 0.8 mm flux densities for several objects on different nights were in good agreement.

We assume that flux densities are dominated by thermal emission from particles, although the combined emission of many molecular lines can also be important at these wavelengths (Sutton et al. 1984). In general, molecular emission becomes increasingly important at shorter wavelengths, owing to the higher density of molecular lines and increasing line opacity with level temperature for these relatively warm disks. Any contribution by molecular lines would tend to *increase* β

TABLE 4

OBSERVED FLUX DENSITIES

HBC ^a	Object	λ_{eff} (mm)	F_{ν} (Jy)	Nights ^b	HBC ^a	Object	λ_{eff} (mm)	F_{ν} (Jy)	Nights ^b
25.....	CW Tau	1.056	0.093 ± 0.026	4	63.....	AA Tau	1.056	0.186 ± 0.034	4
		0.769	0.21 ± 0.04	8			0.769	0.31 ± 0.06	5
28.....	CY Tau	1.056	0.245 ± 0.031	4	65.....	DN Tau	1.056	0.138 ± 0.029	4
		0.769	0.24 ± 0.04	2, 5, 7			0.769	0.38 ± 0.08	5
34.....	RY Tau	1.056	0.354 ± 0.036	4	67.....	DO Tau	1.056	0.194 ± 0.032	4
		0.769	0.58 ± 0.04	1, 5, 7			0.769	0.51 ± 0.10	2, 5
		0.624	0.89 ± 0.14	6, 7			0.624	0.70 ± 0.10	7, 8
35.....	T Tau	1.056	0.417 ± 0.041	4	71.....	GO Tau	1.056	0.146 ± 0.046	4
		0.769	0.91 ± 0.09	1, 3, 5, 7			0.769	0.18 ± 0.06	3, 8
		0.624	1.84 ± 0.25	7			0.624	0.29 ± 0.20	8
37.....	DG Tau	1.056	0.489 ± 0.033	4	72.....	DQ Tau	1.056	0.125 ± 0.030	4
		0.769	0.86 ± 0.10	1			0.769	0.29 ± 0.10	5
		0.624	1.21 ± 0.20	6	74.....	DR Tau	1.056	0.229 ± 0.023	4
41.....	IQ Tau	1.056	0.106 ± 0.031	4			0.769	0.40 ± 0.08	2, 5
		0.769	0.027 ± 0.06	7	77.....	GM Aur	1.056	0.204 ± 0.020	4
		0.624	<0.070	7			0.769	0.85 ± 0.09	1
48.....	HK Tau	1.056	0.110 ± 0.020	4			0.624	1.34 ± 0.33	6
		0.769	0.21 ± 0.03	5, 8	186.....	FU Ori	0.769	0.14 ± 0.11	5
49.....	HL Tau	1.056	1.13 ± 0.02	4	207.....	R Mon	1.056	0.136 ± 0.052	4
		0.769	3.20 ± 0.10	All	243.....	Z CMa	1.056	0.963 ± 0.035	4
		0.624	5.45 ± 0.29	6, 7, 8, 9			0.769	1.60 ± 0.20	5, 8
51.....	V710 Tau	1.056	0.129 ± 0.025	4			0.624	2.69 ± 0.29	6, 8
		0.769	0.19 ± 0.03	5, 9	373.....	V892 Tau	1.056	0.387 ± 0.027	4
		0.624	<0.36	9			0.769	0.95 ± 0.07	2, 3, 5, 7
52.....	UZ Tau	1.056	0.213 ± 0.039	4			0.624	1.31 ± 0.12	7
		0.769	0.74 ± 0.10	2, 5, 7	378.....	V819 Tau	1.056	<0.07	4
		0.624	0.73 ± 0.13	7	384.....	FT Tau	1.056	0.137 ± 0.040	4
54.....	GG Tau	1.056	0.800 ± 0.051	4			0.769	0.25 ± 0.05	3, 8
		0.769	1.25 ± 0.008	1, 5, 7			0.624	0.26 ± 0.10	8
		0.624	1.37 ± 0.17	7	389.....	Haro 6-10	1.056	0.114 ± 0.016	4
58.....	DL Tau	1.056	0.273 ± 0.037	4			0.769	0.51 ± 0.06	8
		0.769	0.53 ± 0.09	1, 7			0.624	1.03 ± 0.45	8
		0.624	0.88 ± 0.14	7	396.....	Haro 6-13	1.056	0.220 ± 0.043	4
61.....	CI Tau	1.056	0.217 ± 0.050	4			0.769	0.46 ± 0.04	3, 8
		0.769	0.85 ± 0.15	2, 5			0.624	0.62 ± 0.12	8, 9
		0.624	1.30 ± 0.21	7					
62.....	DM Tau	1.056	0.206 ± 0.033	4					
		0.769	0.47 ± 0.08	3, 5					
		0.624	0.39 ± 0.13	7					

^a HBC is the Herbig and Bell catalog number.

^b Nights are: (1-6) 1989 Nov 29 through Dec 4; (7-9) 1990 Dec 7 through 9.

beyond its value intrinsic to the particles. CSO CO (2–1) observations of T Tauri stars show antenna temperatures typically around 3 K. The lines are narrow, $\leq 5 \text{ km s}^{-1}$, giving a typical flux of about 450 Jy km s^{-1} . Extrapolating from the case of Orion, where Sutton et al. (1984) suggest that the total contribution to the continuum flux from *all* molecules is approximately 3 times the CO flux, the molecular lines contribute no more than 4% of the total continuum emission on average. For the strongest source, HL Tau, the peak line strength, 8 K, suggests an upper limit of 10% to the molecular contribution.

The particulate mass opacity, κ_v , and its power law index, β , are of primary interest. The index, β , is derived from the observations in two ways. In the first approach, a power law fitted to the flux densities: $F_\nu \propto \nu^\alpha$ gave β directly. If the emission is optically thin, and the temperatures are high enough to make the Rayleigh-Jeans approximation valid for all objects ($T > hv/k \sim 13 \text{ K}$ at 1.1 mm and $\sim 23 \text{ K}$ at $630 \mu\text{m}$), then $\beta_p = \alpha - 2$. (The subscript p will distinguish the emissivity index based on power-law fits from the second method.)

Figure 2 shows five objects with power-law fits to the millimeter-wave flux densities. A primary advantage of the power-law fits is that they do not presume a specific model for the sources (e.g., circumstellar disks) and are in that respect unbiased. The disadvantage is that they will underestimate β if low temperatures or high optical depths contribute substantially to the emission. The results of Paper I indicates that contribution from low temperatures is minor, but a contribution from high optical depths could be substantial, if the particles reside in compact ($R_d \lesssim 100 \text{ AU}$) disks.

The second approach is to calculate the far-infrared and millimeter-wave emission from a thin disk as described in Paper I and fit the long-wavelength spectral energy distributions by varying the parameters of the disk. The advantage of this method is that it gives a more accurate β if the particles do,

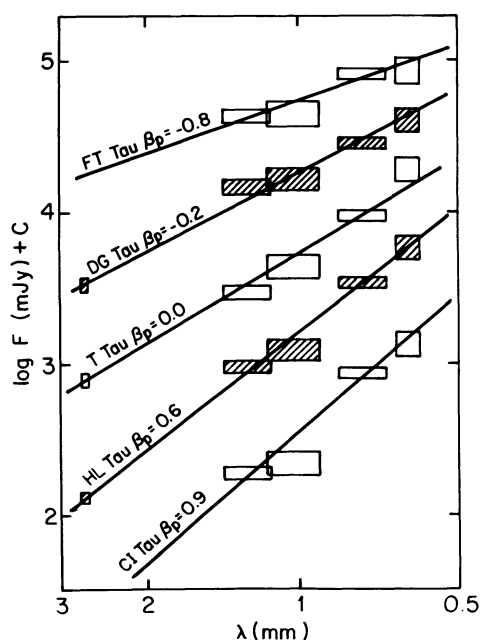


FIG. 2.—Long-wavelength observations for five objects with power-law fits to the flux densities. The width of each box indicates the filter bandwidth; the height indicates 2σ . The constants are: 0 (CI Tau and HL Tau), 1 (T Tau), 1.5 (DG Tau), and 2.50 (FT Tau).

in fact, reside in disks. Corrections for high optical depths and low temperatures in different parts of the disks are specifically included in these calculations (see eq. [22] in Paper I); the emissivity is forced to fit far-infrared and millimeter-wave points simultaneously. Uncertainties introduced through the unknown parameters such as radial density variation and disk outer radius, are generally small, subject to the provisos discussed in § 4.1. The choice of disk mass, M_d , has a strong effect on the values of β derived from the disk calculations. The χ^2 values were calculated on a two-dimensional grid in the parameters β and disk mass, M_p .

Table 5 presents the indices from the disk calculations, expressed as β_d , as well as β_p from the power-law fits. If the opacity coefficient, κ_v , is extrapolated from shorter wavelengths as $\kappa_v = 0.1 (\lambda/250 \mu\text{m})^{-\beta} \text{ cm}^2 \text{ g}^{-1}$, the disk mass, M_p , can be calculated from the millimeter-wave flux densities, and it appears in the fifth column of Table 5. The sixth column gives the parameter Δ defined as the ratio of optically thick to optically thin emission at a wavelength of 1 mm (Paper I) in the calculations. It indicates the validity of assuming low optical depths for circumstellar disks. The unnormalized χ^2 values of the fits appear in the last column.

Because their surface densities are assumed to decrease with increasing distance from the stars, the inner portions of the disks are optically thick even at the longest wavelengths. The calculations require β_d to be larger than β_p to provide good fits to the data. This trend is noticeable in Table 5: β_d is almost always larger than β_p , especially when the fraction of optically thick emission is large ($\Delta \gtrsim 0.5$). In general, the submillimeter data were well fitted by the calculations; the large values of χ^2 (e.g., HL Tau) result from deviations from the far-infrared data, usually at $100 \mu\text{m}$.

As an alternative, we fitted the spectral energy densities with optically *thick* disks, where the variable was the outer radius of the disk, R_d . In these cases, the disks are completely opaque out to $\lambda \sim 3 \text{ mm}$ and subtend uniform (albeit small) solid angles at all wavelengths. For many objects, especially those with $\beta_p \sim 0$, the energy distributions are often consistent with optically thick disks and therefore give no information about β ; only lower limits to the disk masses result from such calculations. Table 6 gives the best-fit radii for optically thick disks along with the χ^2 values for comparison with Table 5.

CY Tau.—CY Tau has a very large millimeter-wave flux relative to the far-infrared points; this was noted in Paper I, and the new submillimeter observations verify the large millimeter-wave flux. To provide a reasonable fit requires a large, optically thick disk with a relatively shallow temperature gradient. A large β produces a marginally better fit to the submillimeter data, but it is poorly constrained.

RY Tau.—The far-infrared spectrum of this object is flat at short wavelengths ($\lambda \lesssim 25 \mu\text{m}$) and falls off steadily from $60 \mu\text{m}$ to 2.7 mm. A disk which becomes optically thin around $30 \mu\text{m}$ with a slightly *negative* β gives an excellent fit to the entire spectrum. By contrast, a small, optically thick disk produces too much far-infrared and too little millimeter-wave emission.

T Tau.—The optically thin disk gives an excellent fit to all except the 2.7 mm point, for which the calculations underestimate the flux density. An optically thick disk produces far too little far-infrared emission relative to the millimeter-wave points; the fit is strikingly poorer overall.

DG Tau.—The submillimeter spectrum of this source is relatively shallow ($\beta_p = -0.23$), yet the far infrared emission is strong. All models have difficulty reconciling these features.

TABLE 5
INDICES FROM THE DISK CALCULATIONS

HBC	Object	β_p	β_d	$\log(M_d)$	Δ	χ^2 ^a
25.....	CW Tau	-0.45 ± 0.25	-0.43 ± 0.26	-2.88 ± 0.16	0.29	4.3
28.....	CY Tau	-0.94 ± 0.25				
34.....	RY Tau	-0.21 ± 0.21	-0.06 ± 0.08	-2.63 ± 0.05	0.25	0.8
35.....	T Tau ^b	0.00 ± 0.07	1.56 ± 0.09	-1.48 ± 0.06	0.31	54
37.....	DG Tau ^b	-0.23 ± 0.07	0.56 ± 0.07	-1.82 ± 0.04	0.35	67
41.....	IQ Tau	0.19 ± 0.25	0.92 ± 0.94	-1.49 ± 0.59	0.48	2.3
48.....	HK Tau	1.08 ± 0.25	1.74 ± 0.45	-1.77 ± 0.28	0.21	4.8
49.....	HL Tau ^b	0.60 ± 0.07	1.21 ± 0.14	-0.95 ± 0.09	0.65	26
51.....	V710 Tau	-0.15 ± 0.25	0.93 ± 0.70	-1.48 ± 0.44	0.48	0.8
52.....	UZ Tau	0.52 ± 0.21	1.15 ± 0.44	-1.19 ± 0.28	0.55	8.1
54.....	GG Tau ^b	0.17 ± 0.07	0.78 ± 0.10	-0.98 ± 0.06	0.85	36
58.....	DL Tau	-0.28 ± 0.21	-0.11 ± 0.29	-1.82 ± 0.18	0.54	8
61.....	CI Tau	0.85 ± 0.21	2.07 ± 0.53	-0.51 ± 0.33	0.65	13
62.....	DM Tau	0.35 ± 0.21	1.02 ± 0.49	-1.42 ± 0.31	0.40	4.1
63.....	AA Tau	0.36 ± 0.25	1.27 ± 0.53	-1.48 ± 0.33	0.36	4.1
65.....	DN Tau	0.89 ± 0.25	2.13 ± 0.89	-0.79 ± 0.56	0.46	6.3
67.....	DO Tau	0.44 ± 0.21	0.92 ± 0.37	-1.82 ± 0.23	0.32	2.2
71.....	GO Tau	-0.48 ± 0.21	0.62 ± 1.79	-1.52 ± 1.12	0.50	0.5
72.....	DQ Tau	0.23 ± 0.25	0.68 ± 1.12	-1.78 ± 0.70	0.39	0.5
74.....	DR Tau	-0.24 ± 0.25	0.57 ± 0.42	-1.88 ± 0.26	0.40	1.7
77.....	GM Aur	0.43 ± 0.21	0.21 ± 0.26	-1.89 ± 0.17	0.38	56
243.....	Z CMa ^c	-0.09 ± 0.48	1.79 ± 0.08	0.58 ± 0.06	0.40	64
373.....	V892 Tau ^b	0.22 ± 0.21	0.24 ± 0.14	-2.43 ± 0.09	0.25	6.3
384.....	FT Tau	-0.84 ± 0.21	-0.80 ± 0.99	-2.77 ± 0.62	0.32	1.0
396.....	Haro 6-13	0.37 ± 0.21	1.14 ± 0.16	-1.78 ± 0.10	0.31	11

^a The fits include all data between 60 μm and 2.7 mm, when available. The target χ^2 values are between 2 and 5.

^b Includes 2.7 mm datum.

^c Assumed distance 1100 pc; $R_d = 2000$ AU; $T_1 = 2020$ K; $q = 0.565$.

The optically thin disk gives a slightly better match, although the resulting submillimeter index is steeper than that observed. The optically thick disk produces too little 100 μm emission,

TABLE 6
BEST-FIT RADII AND χ^2 VALUES FOR OPTICALLY THICK DISKS

HBC	Object	R_d	M_{min} ^a	χ^2
25.....	CW Tau	16.3 ± 1.0	0.016	15
28.....	CY Tau	75.1 ± 5.8	0.3	6
34.....	RY Tau	14.8 ± 0.5	0.01	78
35.....	T Tau ^b	22.8 ± 0.5	0.03	392
37.....	DG Tau ^b	30.6 ± 0.7	0.06	86
41.....	IQ Tau	28.3 ± 2.6	0.05	3
48.....	HK Tau	11.6 ± 0.6	0.01	17
49.....	HL Tau ^b	49.7 ± 0.8	0.16	205
51.....	V710 Tau	27.8 ± 1.5	0.05	2
52.....	UZ Tau	35.3 ± 1.9	0.07	13
54.....	GG Tau ^b	52.5 ± 1.3	0.17	82
58.....	DL Tau	44.7 ± 1.8	0.1	8
61.....	CI Tau	38.3 ± 2.1	0.09	23
62.....	DM Tau	31.2 ± 1.9	0.06	7
63.....	AA Tau	23.3 ± 1.4	0.03	7
65.....	DN Tau	26.5 ± 2.3	0.04	10
67.....	DO Tau	22.2 ± 0.9	0.03	11
71.....	GO Tau	34.9 ± 7.2	0.07	0.5
72.....	DQ Tau	25.2 ± 2.7	0.04	0.7
74.....	DR Tau	25.1 ± 1.9	0.04	0.8
77.....	GM Aur	34.1 ± 1.0	0.05	54
243.....	Z CMa ^c	236 ± 6	3.3	396
373.....	V892 Tau ^b	19.0 ± 0.4	0.02	8.4
384.....	FT Tau	25.3 ± 1.7	0.04	5
396.....	Haro 6-13	22.3 ± 0.8	0.03	50

^a Assumes $\beta = 1$, κ_v as in text.

^b Includes 2.7 mm datum.

^c Assumed distance 1100 pc.

but gives a slightly better match to the long wavelength spectrum.

HK Tau.—An optically thin disk fits all the data beyond 10 μm exceedingly well. The 5 and 10 μm points are low, possibly implying a gap in the particle distribution at small radii. An opaque disk is underluminous in the far-infrared, relative to the observations, and fails to fit the millimeter-wave slope.

HL Tau.—HL Tau is one of the most luminous submillimeter objects in Taurus, and is expected to have both a large disk mass and large accretion rate. The optically thin disk gives an excellent fit to the data (note: the stated far infrared uncertainties for this bright object probably underestimate the true uncertainties, since the *IRAS* beam size is rather large). The optically thick disk gives inadequately low infrared emission, does not match the slope of the submillimeter spectrum, and predicts about twice as much emission at 2.7 mm as is actually observed. This bright object is one of the better examples of a source for which the optically thin assumption generates a significantly better match to the data.

GG Tau.—The submillimeter and millimeter-wave points have a slight downward curvature toward long wavelengths. By itself, this indicates an optically thick model will not fit well. The optically thin emission fits the data well at all points from 60 μm to 2.7 mm. The optically thick disk fits the 60 to 600 μm points well, but gives too shallow a slope to fit the longer wavelength points. It predicts more 2.7 mm emission than is observed.

CI Tau.—The 1.1 mm flux density is too low to be consistent with the 1.3 mm and 800 μm observations; all fits suffer as a result. The optically thin disk model actually requires $\bar{\tau} \sim 1$ out to 800 μm , to give a good fit. It differs from the optically thick model only in giving a slightly better 800 μm to 1.3 mm

slope. A completely opaque disk gives too little 600 μm emission and too much 1.3 mm emission.

DO Tau.—The optically thin disk fits the data very well at all points. The optically thick disk produces too little 100 μm flux (but the uncertainty is large) and too shallow a submillimeter spectrum; the difference is only marginally significant.

GM Aur.—GM Aur also has a low 1.1 mm flux density relative to the 1.3 mm and 800 μm points. The optically thin and thick disks fit the data almost equally well, judging from a visual inspection of the curves.

Z CMa.—The large far-infrared flux densities compared to those in the submillimeter region almost require an optically thin disk. The submillimeter spectral index is, nevertheless, quite shallow, and the optically thin model gives a submillimeter index which is larger than apparent from the submillimeter points alone. However, the optically thick disk cannot give an acceptable fit to the data; the calculated far-infrared flux is much smaller than that which is observed, and it is constrained strongly by the submillimeter data. Like HL Tau, Z CMa is a good example of a luminous source with an optically thin disk.

V892 Tau.—Also known as Elias 1, V892 Tau has a 100 μm flux density which is probably contaminated by a source to the north; we used only an upper limit at this wavelength. Both optically thin and thick disks give acceptable fits to the data.

Haro 6-13.—An optically thin disk produces an excellent fit to all data points, and the submillimeter spectral index is greater than 0 ($\beta_p \sim 0.4$). The optically thick disk not only gives the wrong slope near 1 mm, it produces somewhat too little 100 μm flux to match the observations. The far-infrared and millimeter-wave flux densities have small uncertainties, hence the large difference in χ^2 between the two models.

4. DISCUSSION

The principal difficulty in deriving β and, thus, the particle properties, is the unknown opacity in the circumstellar material. If the typical object has a small millimeter-wave opacity, the *observed* spectral index by itself is sufficient to derive β through the power-law fits; the distribution of temperatures implied by the far-infrared emission, coupled with the low visual extinction to these objects, makes it unlikely that substantial amounts of cool matter contribute to the emission, i.e., $h\nu/k \ll T$ (Paper I). Unfortunately, the optical depth for a given mass is not always well-determined, because the source size is unknown.

The vast majority of the sample stars have apparent emissivity indices less than or equal to 1, even when β is derived from the disk calculations. Figure 3 shows histograms of the best-fit values of β . The power-law indices, β_p , show a marked peak near 0 and no sources with $\beta_p > 1$. The disk calculations indicate $\beta_d \leq 1$ in most cases, with about 25% of the objects having larger values. Only two of 25 objects have $\beta_d \sim 2$ consistent with standard notions about grains in the interstellar medium (see Hildebrand 1983; Draine & Lee 1984; Emerson 1988; Draine 1989).

Figure 4 includes only those objects which *cannot* be fitted by optically thick disks. The distribution of β -values shifts toward larger values. Only objects with $\beta_p \lesssim 1$ can be reasonably consistent with high opacities. Nevertheless, there are still many sources with low β_p which cannot be fitted by optically thick disks. A comparison of the χ^2 values between Tables 5

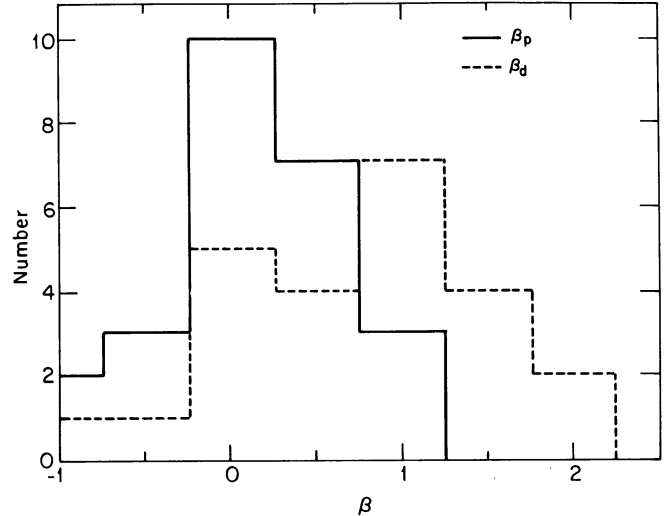


FIG. 3.—Histogram of β , the power-law indices for the particle emissivities.

and 6 shows that in almost all cases optically thick disks are poorer fits to the data than the optically thin model.

We believe the most natural explanation for the results is that, for the objects considered here, β is smaller than is usually assumed for interstellar particles at wavelengths longward of about 100 μm . Similar conclusions were reached by Adams et al. (1990) and Weintraub et al. (1989) based power-law fits to submillimeter data.

In the next subsection, we discuss the uncertainties in β and κ , introduced by unknown opacity effects, and the likely constraints imposed by other data (e.g., observations of the gas). Section 4.2 concentrates on the physics of small grain emission with an eye toward understanding the connection between κ , and particle properties. The particular case of circumstellar disks is addressed in § 4.3. Throughout, values of κ will refer to total mass in gas and particles, even though the opacity is produced entirely by the solid particles.

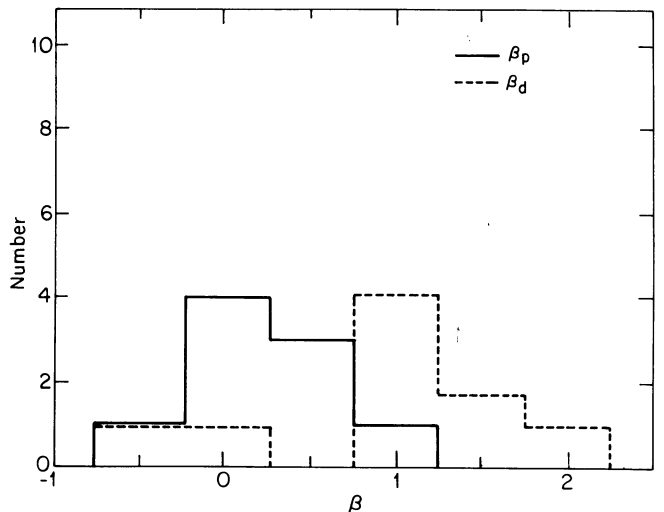


FIG. 4.—These histograms are similar to those of Fig. 3, but they include only objects which *cannot* be fitted with optically thick disks.

4.1. Disk Opacity and the Spectral Index

Paper I describes the calculations of emission from a thin disk. The important parameters are the disk mass, M_D , the outer radius, R_D , the inclination angle to the line of sight, θ , the mass opacity, κ_v , and the power-law indices describing the radial variations of density (p) and temperature (q), e.g., $T \propto r^{-q}$. Our conclusions here about opacity effects do not depend strongly on the assumption of power-law forms for the density and temperature variations. We showed in Paper I that the approximate relation between the observed spectral index, α , and the emissivity index, β , is:

$$\alpha \approx 2 + \frac{\beta}{1 + \Delta}, \quad (1)$$

where Δ is the ratio of optically thick to optically thin emission from the disk, and the spectral index refers to the flux density F_ν rather than to the spectral energy density νF_ν .

It is useful to define several characteristic quantities associated with the disk: r_0 is the inner disk radius, $\bar{\tau}_v$ is the average optical depth in the disk, and r_1 is the radius at which the optical depth is unity. Then

$$\bar{\tau}_v = \frac{\kappa_v M_D}{\pi R_D^2 \cos \theta}, \quad (2)$$

$$r_1 = R_D \left[\bar{\tau} \left(\frac{2-p}{p} \right) \right]^{1/p}, \quad (3)$$

$$\Delta = \frac{1}{\bar{\tau}_v R_D^p} \frac{p}{2-p} \frac{2-p-q}{2-q} \frac{r_1^{2-q} - r_0^{2-q}}{R_D^{2-p-q} - r_1^{2-p-q}}. \quad (4)$$

For all disks of interest here, $2 - q > 0$ and $r_1 \gg r_0$, so we may ignore r_0^{2-q} . The exponent $2 - p - q$ may be positive or negative; it is often taken to be zero in disk calculations (e.g., $p = 1.5$, $q = 0.5$).

After a little algebra, one can write Δ in two alternative forms, depending on the value of $\gamma \equiv (2 - p - q)/p$:

$$\Delta = \frac{\bar{\tau}_p^\gamma}{1 - \bar{\tau}_p^\gamma} \frac{2-p-q}{2-q} \quad (\gamma \neq 0), \quad (5)$$

$$\Delta = \frac{1}{\ln(1/\bar{\tau}_p)} \quad (\gamma = 0). \quad (6)$$

where $\bar{\tau}_p \equiv \bar{\tau}_v [(2-p)/p]$. The approximations used here are valid only for $\bar{\tau}_p < 1$, which will be adequate for this discussion. In both equations, Δ becomes very large and approaches infinity as $\bar{\tau}_p$ approaches unity, and the entire disk becomes optically thick to radiation at frequency ν .

It is evident that arbitrarily large values of β can be consistent with any observed α . Consider, for example, the case $\gamma = 0$ and $\bar{\tau}_p$ close to unity. Equation (1) becomes

$$\begin{aligned} \alpha &\approx 2 + \frac{\beta}{1 + [\ln(1/\bar{\tau}_p)]^{-1}}, \\ &\approx 2 - \beta \ln(\bar{\tau}_p). \end{aligned} \quad (7)$$

The exact form of this equation is not strictly valid for $\bar{\tau}_p$ very close to unity, where the approximations used in the derivation begin to break down. But the essential point is that the observed spectral index, α , reflects the *product* of β with the logarithm of M_D , not β itself. The uncertainties in β create correspondingly larger uncertainties in M_D . For this reason, log M_D is given in Table 5.

For an optically thick disk in the Rayleigh-Jeans limit, the flux density is

$$F_\nu = \frac{1}{2-q} \frac{\pi R_D^2}{D^2} \frac{2kT(R_D)\nu^2}{c^2} \cos \theta, \quad (8)$$

where we assume the inner radius is negligibly small and D is the distance to the source. Following the conventions of Paper I, the outer radius needed to produce flux density F_ν is

$$R_D = \left(\frac{2-q}{\pi r_1^2} \frac{D^2 c^2}{2k\nu^2} \frac{F_\nu}{T_1 \cos \theta} \right)^{1/(2-q)} \text{ AU}, \quad (9)$$

with $r_1 = 1$ AU. The minimum mass needed to produce an optically thick disk derives from the condition $\tau = 1$ at $r = R_D$:

$$M_D \gtrsim 2 \frac{2-p}{2-q} \frac{D^2 F_\nu}{\kappa_v \cos \theta} \frac{c^2}{\nu^2} \frac{1}{2kT(R_D)}. \quad (10)$$

Although the values of R_D and M_D appearing in Table 6 were calculated numerically—so that neither the Rayleigh-Jeans approximation nor the assumption of vanishingly small inner radius were required—the analytic approximation provided a useful check on the results. In all cases, equations (9) and (10) reproduce the results almost exactly.

One can see from the equations that R_D is well-constrained by the submillimeter flux densities. Typical values of q are between 0.5 and 0.75, so that $R_D \propto F_\nu^{0.7}$ (the values of T_1 are strongly constrained by far infrared flux densities). An optically thick disk would need to have a fairly sharp boundary to be consistent with the observed flux densities over a range of frequencies.

4.2. Emission Efficiency: Particle Composition

The mass opacity coefficient, κ_v , is usually written

$$\kappa_v = \frac{3}{4a} \frac{1}{\rho} Q_{\text{em}}, \quad (11)$$

where Q_{em} is the emission efficiency of individual particles, ρ (g cm^{-3}) is the density, and $3/4a$ is the geometrical cross section to volume ratio for the particles for spheres of radius a (Hildebrand 1983). The long-wavelength behavior of Q_{em} is proportional to $a\nu^2$ for both crystalline and metallic spheroids (Bohren & Huffman 1983), and also for amorphous solids of spheroidal shape (Seki & Yamamoto 1980). Since the frequency dependence is nicely consistent with the sum rule derived by Purcell (1969; see also Emerson 1988), it is commonly assumed that $\beta = 2$ for interstellar particles at long wavelengths (e.g., Draine & Lee 1984).

Particle size can modify the dielectric properties of the grains, if the grains are conducting. If the ratio of surface area to volume is large, as it will be for very small grains, then $Q_{\text{FIR}} \propto \nu$ (Seki & Yamamoto 1980; Emerson 1980). Effectively, the volume absorption is diminished and small values of β result from a *decrease* in the short wavelength opacity.

Pollack et al. (1991) suggest that common astrophysical materials, especially iron and silicon compounds can easily produce a low β behavior at long wavelengths. They estimate that troilite (FeS) has sufficiently strong translational lattice modes to produce $\beta \lesssim 0$ out to wavelengths ~ 1 cm. Their work specifically treats the chemistry of particles in circumstellar disks and is directly applicable to the observations at hand.

The long wavelength emissivity may also be increased through shape effects alone. Any deviation from sphericity will

raise the ratio of surface area to volume and, hence, the long-wavelength coupling. While shape-dependent opacity effects usually are strong only in the long wavelength limit for conducting materials, such as iron or graphite, these materials are reasonable abundant in interstellar gas. Various distributions of graphite needles, for example, can provide any β between 0 and 2 (Wright 1982); in all cases, the magnitude of κ_v is enhanced at wavelengths near 1 mm. Prolate or oblate spheroids of FeS with axial ratios of 4:1 will increase κ_v by factors of 3 at 1 mm (Pollack et al. 1991).

Fractal grains, in particular, can greatly enhance submillimeter emission of conducting particles for a fixed grain volume. The surface area of these fluffy aggregates increases faster than $N_a^{2/3}$, where N_a is the number of constituents (atoms or clusters of atoms). Wright (1987) has shown that fractal particles only a few microns in maximum dimension have high opacity out to around 1 mm wavelength; $\beta \approx 1$ over about 2 decades in wavelength for a single-size fractal (see Koike, Hasegawa, & Manabe 1980, and references therein). It is noteworthy that Meakin & Donn (1988) expect fractals under the conditions in the primitive solar nebular. However, the essential point here is that $\beta \lesssim 1$ behavior is *not* difficult to produce with materials thought to be abundant in the interstellar medium.

4.3. Particle Opacity in Circumstellar Disks

The value of the bulk opacity, κ_v , bears most strongly on the relationship between disk physical properties, such as mass, and observable characteristics, such as spectral energy distribution. However, particle growth and chemical reactions peculiar to the dense, warm environment in the primitive solar nebula undoubtedly give rise to conditions atypical of the general interstellar medium. We believe, therefore, that studies of the mass opacity coefficient for interstellar dust provide little guide to the values of κ_v and β appropriate to the circumstellar disks considered here. In any case, there are many pitfalls in determining κ_v for the interstellar medium; the considerable disparity between the numerous results (Werner et al. 1976; Harvey, Hoffman, & Campbell 1978; Schwartz 1982; Hildebrand 1983; Rowan-Robinson 1986; Draine 1989; Page et al. 1990) arises largely from the tenuous connection between the physical quantities— κ_v and β —and the actual observables—antenna temperature and flux density.

Section 4.1 showed that while multiwavelength observations of disks can provide a measure of the spectral index, α , they do not necessarily constrain the upper bound to β . For this purpose, some independent determination of the disk mass, M_D , is needed. For a few of these stars, M_D has been derived from observations of the molecular gas. Sargent & Beckwith (1987, 1991) estimate $M_D \approx 0.1 M_\odot$ from ^{13}CO observations of HL Tau. Unfortunately, these estimates are also lower limits because of optical depth uncertainties in the molecular transitions. In principle, M_D may be constrained by observations of emission from optically thin species in the disks, for example $^{13}\text{C}^{18}\text{O}$. Such observations are unavailable for any of the objects in this sample. Alternatively, the fact that the gas around HL Tauri appears to be gravitationally bound to the star can be exploited to provide a mass estimate; the disk mass must be $\leq 0.5 M_\odot$ (Sargent & Beckwith 1987), so that $\beta \leq 2$.

The observations presented here are insufficient to rule out optically thick disks in most sources. In our opinion, however, the submillimeter emission is likely to be optically thin in

almost all cases for several reasons. Opaque disks yield systematically poorer fits to the data for the majority of sources, especially those in which the wavelength coverage is very broad. Some of the most luminous disks in our sample are probably optically thin (RY Tau, T Tau, HL Tau, and Z CMa), judging by the goodness of the fits. If, as commonly believed, the luminosity derives from high mass-accretion rates, these disks should have a greater tendency toward high opacities than the other sources. We know of no mechanism to sharply limit the outer radii of the disks, and at least a few are observed to have substantial gas ~ 1000 AU or more from the stars (Sargent & Beckwith 1987, 1991).

If we are correct, our observations imply that $\beta \lesssim 1$ characterizes the particle emissivity in these disks. The derived indices fall almost entirely within the range $\beta < 2$. Including objects from Weintraub et al. (1989) and Woody et al. (1989), only a few stars in a sample of about 30 have steeper spectra.

Of the various ways to bring about $\beta < 2$, particle shape changes or changes in chemistry would equally serve to produce the observed effect. In either case, κ_v would be enhanced relative to the values commonly adopted for the interstellar medium. To date, values of κ_v of order 0.002–0.004 have been favored by various groups (Hildebrand 1983; Draine & Lee 1984; Draine 1989; Adams et al. 1990). We have suggested (Paper I; Beckwith & Sargent 1991), that $0.02(1 \text{ mm}/\lambda) \text{ cm}^2 \text{ g}^{-1}$ provides a better fit to the long-wavelength spectra (assuming $\beta = 1$), while maintaining the normalization established by Hildebrand at $250 \mu\text{m}$ for molecular clouds. If particle shapes, such as fractals, dominate κ_v (Wright 1987), this normalization is probably appropriate. If composition changes alter β (Pollack et al. 1991), the extrapolation is invalid, and κ_v must be estimated from first principles.

Specific estimates of κ_v depend on the adopted grain model. We estimate that a collection of graphite needles (see Wright 1982) with lengths between 0.5 and $20 \mu\text{m}$ would give $\kappa_v(1 \text{ mm}) \approx 3(1 \text{ mm}/\lambda) \text{ cm}^2 \text{ g}^{-1}$, assuming the appropriate mass in gas. Even if the graphite needles constitute only a few percent of the total particle mass, they might still dominate the long-wavelength opacity. Alternatively, for a distribution of different size fractals, Wright's (1987) calculations yield $\kappa_v \approx 3(1 \text{ mm}/\lambda) \text{ cm}^2 \text{ g}^{-1}$. Fractals have the further advantage that the collective β in a disk is only a weak function of the particle size distribution. Pollack et al. (1991) derive $\kappa_v \sim 0.006 \text{ cm}^2 \text{ g}^{-1}$ at 1 mm for spherical troilite grains with a factor of 3 uncertainty in either direction; ellipsoidal shapes tend to increase κ_v by factors of a few.

A variety of effects can give submillimeter opacities with $\beta < 2$. Even if a small fraction of the particle mass resides in these high opacity particles, they might still dominate the overall opacity and raise the mass opacity coefficient. It is very difficult to adequately calculate κ_v from first principles with any confidence. However, we are optimistic that it might be determined from the right combination of observations. Interferometric maps of the gas in optically thin transitions of the abundant molecules (e.g., CO) can, in principle, give accurate measures of the disk mass and its radial distribution. Spatially resolved millimeter-wave continuum maps will, when combined with the temperatures gleaned from infrared emission, give the distribution of optical depth. In combination, these observations will give κ_v directly. It will then be possible to discuss the issue of shape or composition changes with some confidence and address the issue of particle growth prior to vigorous planet formation.

5. CONCLUSIONS

We have observed submillimeter flux densities from the circumstellar disks around 29 pre-main-sequence stars. The properties of these disks are of special interest, because they bear many similarities to those of the primitive solar nebula. Studies of such systems may therefore lead to a better understanding of the formation of planetary systems like our own.

Critical factors in determining the mass of these disks are the millimeter-wave mass opacity coefficient, κ_v , and the index of its power-law frequency dependence, β . These quantities have been studied extensively in molecular clouds and the diffuse interstellar medium, but the results are often widely discrepant. Moreover, these derivations of κ_v and β may well be inappropriate to the case of circumstellar disks.

Since the emission from many objects in our sample is likely to be optically thin at submillimeter wavelengths, measurement of the flux density distributions in this regime should, in principle, provide a means of establishing β for circumstellar disks. We show that for most of our objects, the emissivity index, β is unity or less. Larger values could obtain only if the disks were optically thick. We believe this result shows that the *intrinsic* value of β is unity or smaller.

A number of authors (see § 4.2) have suggested circumstances which could readily produce $\beta \approx 1$. In the disks considered here, several requisite criteria can be met. The presence of a population of nonspherical particles such as fractal grains (e.g., Wright 1982, 1987) seems to us an attractive explanation

for our results. Particle growth, and even the presence of fractal grains (Meakin & Donn 1988) are anticipated phenomena in preplanetary disks. Alternatively, changes in composition, especially the formation of iron-bearing compounds, could completely dominate the submillimeter opacities even for spherical particles.

At present, there is no simple way to establish the bulk opacity coefficient, κ_v , even in the relatively straightforward case of disks around young stars. Observations of the spectral energy distribution of the circumstellar particulate matter are not in themselves sufficient to establish either β or κ_v , unambiguously. There is every indication that their values are different than in molecular clouds or the diffuse interstellar medium. Where independent mass determinations for the disks are available, in molecular lines, for example, both *can* be constrained. The way will then be open for the investigations of particle size, composition, and distribution critical to studies of the early solar system.

We are grateful to J. Keene for advice about the bolometer system. We thank A. Schinkel, L. Strom, and K. Young for valuable assistance at the telescope, and E. L. Wright, A. J. Sievers, J. Pollack, and J. R. Houck for discussions concerning the emissivity properties of small particles. We thank an anonymous referee for providing several suggestions which improved this paper. Support for this research came from NSF grant AST 8802458 to Cornell and NSF grant AST 9015755 to Caltech.

REFERENCES

- Adams, F. C., Emerson, J. P., & Fuller, G. A. 1990, *ApJ*, 357, 606
 Beckwith, S. V. W., Sargent, A. I., Chini, R. S., & Güsten, R. 1990, *AJ*, 99, 924 (Paper I)
 Beckwith, S., Sargent, A. I., Scoville, N. Z., Masson, C. R., Zuckerman, B., & Phillips, T. G. 1986, *ApJ*, 309, 755
 Bohren, C. F., & Huffman, D. R. 1983, *Absorption and Scattering of Light by Small Particles* (New York: Wiley)
 Cunningham, C. T. 1982, Ph.D. thesis, University of London
 Draine, B. T. 1989, in *Proc. of the 22d ESLAB Symposium on Infrared Spectroscopy in Astronomy*, ed. B. H. Kaalich (Noordwijk: ESA Publications), 93
 Draine, B. T., & Lee, H. M. 1984, *ApJ*, 285, 89
 Emerson, J. P. 1988, in *Formation and Evolution of Low Mass Stars*, ed. A. K. Dupree & M. T. V. Lago (Dordrecht: Kluwer), 21
 Harvey, P. M., Hoffmann, W. F., & Campbell, M. F. 1978, *A&A*, 70, 165
 Hildebrand, R. H. 1983, *QJRAS*, 24, 267
 Koike, C., Hasegawa, H., & Manabe, A. 1980, *Ap&SS*, 67, 495
 Meakin, P., & Donn, B. 1988, *ApJ*, 329, L39
 Page, L. A., Cheng, E. S., & Meyer, S. S. 1990, *ApJ*, 355, L1
 Pollack, J. B., Hollenbach, D., Simonelli, D., Beckwith, S., Roush, T., & Fong, W. 1991, in preparation
 Purcell, E. M. 1969, *ApJ*, 158, 433
 Rowan-Robinson, M. 1986, *MNRAS*, 219, 737
 Sargent, A. I., & Beckwith, S. V. W. 1987, *ApJ*, 323, 294
 ———. 1989, in *IAU Colloquium 120, Structure and Dynamics of the Interstellar Medium*, ed. Tenorio-Tagle, J. Melnick, & M. Moles (Berlin: Springer), 215
 ———. 1991, in preparation
 Schwartz, P. R. 1982, *ApJ*, 252, 589
 Seki, J., & Yamamoto, T. 1980, *Ap&SS*, 72, 79
 Sutton, E. C., Blake, G. A., Masson, C. R., & Phillips, T. G. 1984, *ApJ*, 283, L41
 Weintraub, D. A., Sandell, G., & Duncan, W. D. 1989, *ApJ*, 340, L69
 Werner, M. W., Gatley, I., Harper, D. A., Becklin, E. E., Lowenstein, R. F., Tesesco, C. M., & Thronson, H. A. 1976, *ApJ*, 204, 420
 Whitcomb, S., & Keene, J. 1980, *Appl. Optics*, 19, 197
 Woody, D. P., Scott, S. L., Scoville, N. Z., Mundy, L. G., Sargent, A. I., Padin, S., Tinney, C. G., & Wilson, C. D. 1989, *ApJ*, 337, L41
 Wright, E. L. 1982, *ApJ*, 255, 401
 ———. 1987, *ApJ*, 320, 818